



OPEN Integrating transcriptome and metabolome analyses to characterize flower development in *Salix variegata* Franch., a typical dioecious plant

Huan Zhang, Wenqiao Li, Xiao Zhang, Rui Pan, Mingwei Tang, Yang Peng, Yiyun Wang, Youwei Zuo, Zhe Zhang & Hongping Deng✉

Salix variegata, a typical dioecious plant with high reproductive and adaptive ability, has important ecological and ornamental value. To understand the potential mechanisms and metabolite dynamics of male and female flowers development, the first comparative analysis of the transcriptome and metabolome of *S. variegata* was applied. As a result, 12,245 differentially expressed genes (DEGs) and 4,145 differently expressed metabolites (DEMs) were identified. Transcriptomic analysis showed that the male and female flowers development processes were related to phenylpropanoid and flavonoid biosynthesis. According to the metabolic profile, the main amino acids, flavonoids, phenylpropanoids, and their derivatives were accumulated during the development of male and female flowers of the *S. variegata*. Combined transcriptomic and metabolomic analyses indicated that the *AUX/IAA*, *bHLH*, *MYB*, *ERF* and *RLK* transcription factors (TFs) and their associated key DEGs may mediate the metabolism of phenylpropanoids and flavonoids, which in turn regulate the development of male and female flowers in *S. variegata*. These results provide important insights to elucidate the development of male and female flowers of *S. variegata* at the molecular level. Our results will contribute to understanding the molecular and genetic mechanisms of male and female flower development in typical dioecious plants.

Keywords *Salix variegata* Franch., Flower development, Transcriptome, Metabolome, Coexpression network

Plants are extremely important to the survival of human beings, as they can purify the air to produce oxygen, solve the problem of food sources for human beings, and cure human diseases, so exploring the biological mechanisms of plants is crucial to the survival and development of human beings. Previously, studies on the complex biology of plants mainly focused on their morphology, physiology, and biochemistry, and later began to analyze their intrinsic molecular mechanisms using a single-omics approach^{1,2}. Gradually, it has been found that it is difficult to fully characterize complex plant biological processes by a single genomics technique, and given this, a variety of combined genomics research techniques have been developed. By integrating information from different groups, the multi-omics approach can help people understand the regulation and causality between molecules by exploring the candidate key factors at a deeper level³.

Plant growth and development is a highly complex process that involves the formation of various tissues and organs, color formation, and quality formation. For higher plants, flowering is an important part of their life history and is aimed at producing seeds and transmitting genetic information. Flower development is a prerequisite for successful sexual reproduction in plants, whether self-pollinated or cross-pollinated, and is regulated by the external environment⁴. The process of flower development in higher plants is the growth and development of plants to a certain stage, under the action of temperature, light, and other environmental factors, the hormones related to the regulation of flower bud differentiation continue to accumulate in the plant, and under the action of these hormones the meristematic tissue undergoes a series of morphological, structural and physiological changes, and its nutritive growth is aligned to no longer be transformed into leaf buds but rather to

School of Life Sciences, Southwest University, Beibei District, Chongqing 400715, China. ✉email: denghp@swu.edu.cn

flower buds⁵. In recent years more and more genes and TFs related to flower development have been identified, such as *AP2/ERF*, *MYB*, *bHLH*, *MADS-box*, *NAC*, *FAR1*, *TERF*, *Tify*, and *WRKY*^{6–13}. These genes are responsible for the transformation of the plant's stem-tip meristematic tissues to flower buds, then to the full bloom, final bloom, and finally to the formation of seeds.

Salix variegata Franch. belonging to the Salicaceae family, is a typical dioecious plant, flood-resistant, drought-resistant, and resistant to heavy metal stress, it is an excellent soil-fixing and dike protection plant, but also has great ecological restoration potential^{14,15}. *S. variegata* is widely distributed in eastern Tibet, northern Yunnan, Guizhou, Sichuan, Chongqing, and southeastern Gansu in China, and often grows at riverbanks in sandy soils, pebble fields, and between rock crevices¹⁶. River levels subside, and plants in the riparian zone experience alternating annual stresses of flooding and drought, which also affects the growth and development of plants in the riparian zone^{17–19}. As a dominant species in the riparian zone, *S. variegata* is well adapted to changes in water levels in the riparian zone. Previous researchers have conducted many studies around its ecological adaptations, such as seed germination, physiology, and biochemistry under flooding stress, reproduction, morpho-physiological adaptations under heavy metal cadmium stress, soil microorganisms under double flooding-cadmium stress, physiological and biochemical characteristics, and transcriptional and metabolic traits of *S. variegata* under flooding stress^{15,20–27}. Although many studies have been conducted on *S. variegata*, few have explored the underlying molecular mechanisms of its ecological adaptations. It has been found that *S. variegata* can rapidly recover its growth after flooding, and it can flower and fruit normally, its seed activity is also strong²⁸. *S. variegata*, as a typical dioecious plant, generally flowers from June to December. However, there is little available information on the molecular mechanisms and metabolic dynamics of its male and female flower development. In this study, transcriptomic and metabolomic techniques were used to characterize the transcriptome and metabolome of *S. variegata* during male and female flowers development. This study had the following two main objectives: (1) to investigate the regulatory pathways and genes involved in the development of male and female flowers in *S. variegata*, and (2) to determine the dynamics of metabolites during the development of male and female flowers in *S. variegata*. This study intends to provide a basis for further research on sexual reproduction and breeding of *S. variegata* and even dioecious plants by elaborating, for the first time, the molecular genetic mechanism of male and female flowers development in *S. variegata*.

Results

Transcriptome variations at different developmental stages of *S. variegata* male and female flowers

Sequencing of 18 cDNA libraries constructed from three different floral developmental stages of *S. variegata* male and female flowers yielded a total of 114.85 Gb of clean data, with more than 5.92 Gb of clean data and Q30 ≥ 94.65% for each sample (Supplementary Table S1). Principal component analysis (PCA) results showed that the different groupings of samples could be differentiated from each other and that the male and female flowers showed similar expression patterns at the same floral stage of *S. variegata*, with PC1 (23.11%) and PC2 (11.64%) separating the two (Supplementary Fig. S1A).

A total of 12,245 DEGs were screened by Fold Change (FC) ≥ 1.5, False Discovery Rate (FDR) < 0.01 (Supplementary Table S2). Among them, there were 2,372, 1,232, and 1,103 DEGs in F1 vs. F2, F1 vs. F3, and F2 vs. F3, respectively. 6,981, 6,684, and 1,003 DEGs were found in M1 vs. M2, M1 vs. M3, and M2 vs. M3, respectively. 517, 4,982, and 2,587 DEGs were found in F1 vs. M1, F2 vs. M2, F3 vs. M3, respectively. Among the three comparison groups of female flowers, the F1 vs. F2 screened the most DEGs, with 1,323 up-regulated genes and 1,049 down-regulated genes, indicating that more genes are involved in the development of female flowers of *S. variegata* from bud to anthesis, while the F2 vs. F3 screened the fewest DEGs, with 1,103 DEGs. Among the three comparison groups of male flowers, the M1 vs. M2 screened the most DEGs, with 3,812 up-regulated genes and 3,169 down-regulated genes, suggesting that more genes are involved in the development of *S. variegata* male flowers from flower bud to anthesis, while the M2 vs. M3 had the fewest DEGs, with 1,003 DEGs. In the comparison group of male and female flowers at the same flowering stage, DEGs were most abundant in F2 vs. M2 (4,982), containing 2,464 up-regulated and 2,518 down-regulated genes, and least abundant in F1 vs. M1 (517), with 162 up-regulated genes and 355 down-regulated genes. Male and female flower DEGs were categorized separately using Venn diagrams. There were 20 DEGs shared among the three periods of female flowers, with 1,281, 374, and 650 specifically expressed DEGs in F1 vs. F2, F1 vs. F3, and F2 vs. F3, respectively. 383 DEGs shared among the three periods of male flowers, with 2,208, 1,680, and 81 specifically expressed DEGs in M1 vs. M2, M1 vs. M3, and M2 vs. M3, respectively. 54 DEGs shared among the three comparison groups of male and female flowers at the same flowering stage, and 292, 3,646, and 1,300 specifically expressed DEGs in F1 vs. M1, F2 vs. M2, and F3 vs. M3, respectively (Fig. 1A–C).

The clustering heat map was able to provide an overall picture of the expression of DEGs in different developmental stages of *S. variegata* male and female flowers. As can be seen from the figure, both male and female flowers of *S. variegata* showed significant differences in the expression of different genes and different developmental stages, and the biological replicates were highly similar among the groups (Supplementary Fig. S1B). The expression of genes was categorized into three clusters in total, with the first cluster of genes being more highly expressed at the bloom stage of male flowers and least expressed at the bud stage of male flowers. The genes in the second cluster were most highly expressed at the bloom stage of female flowers and least highly expressed at the terminal flower stage of male flowers. The third cluster of genes had the highest expression at the bud stage of male flowers and the lowest expression at the final flower stage of male flowers. The expression of cluster I and cluster II genes tended to increase with flower development in F, and the expression of cluster III genes tended to decrease with female flower development. The expression of cluster I genes first increased and then decreased with the development of male flowers, and the expression of cluster III genes gradually decreased with the development of male flowers.

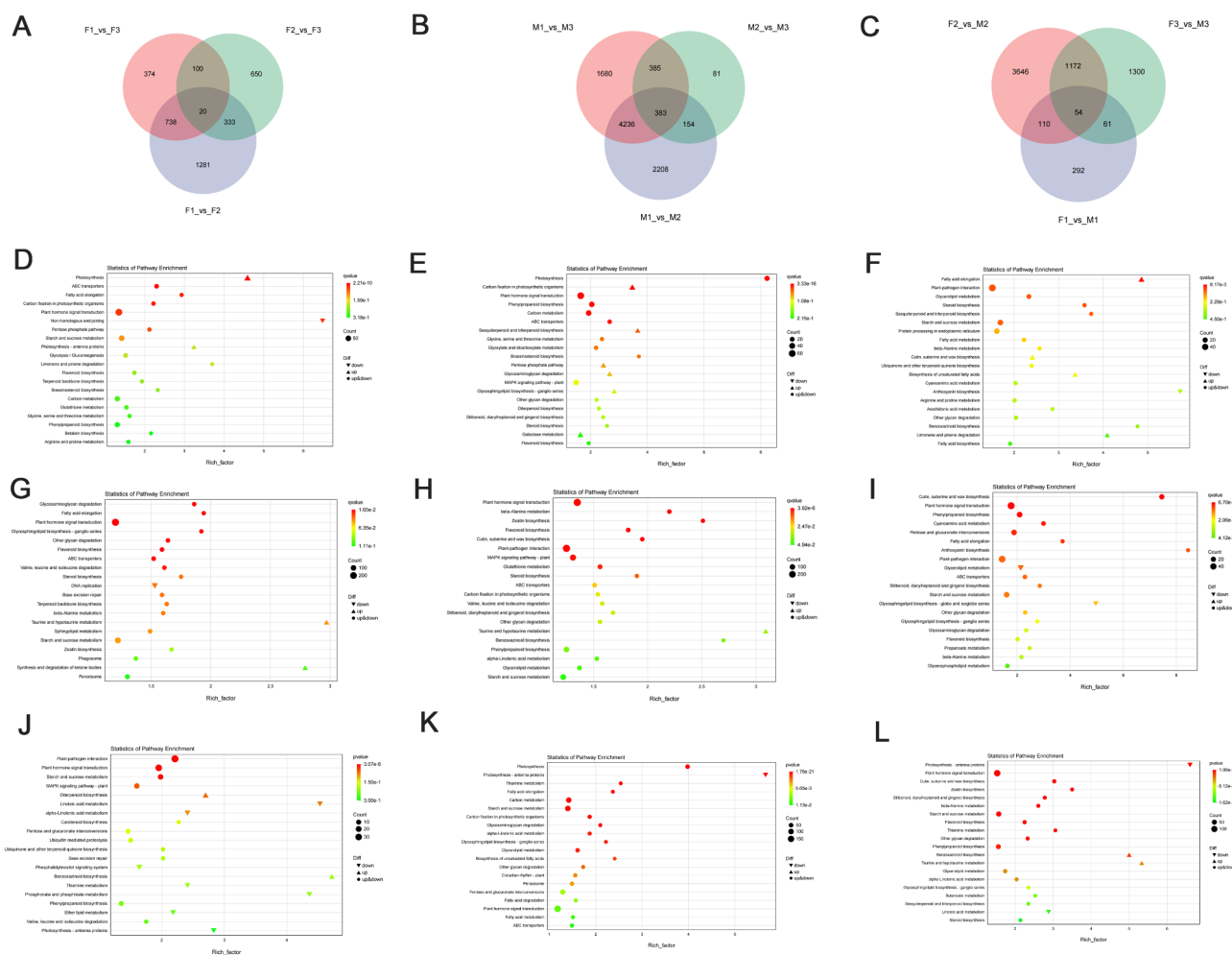


Fig. 1. Characterization of DEGs for three periods of *S. variegata* male and female flowers (A) Venn diagram of DEGs for three comparison groups of *S. variegata* female flowers, (F1) flower bud stage, (F2) full bloom stage, and (F3) final bloom stage. (B) Venn diagram for three comparison groups of *S. variegata* male flowers, (M1) flower bud stage, (M2) full bloom stage, (M3) final bloom stage. (C) Venn diagram for the three comparison groups of male and female flowers at the same flowering stage. (D) KEGG pathway enrichment analysis of DEGs in F1 vs. F2 groups. (E) KEGG pathway enrichment analysis of DEGs in the F1 vs. F3 group. (F) KEGG pathway enrichment analysis of DEGs in the F2 vs. F3 group. (G) KEGG pathway enrichment analysis of DEGs in the M1 vs. M2 group. (H) KEGG pathway enrichment analysis of DEGs in the M1 vs. M3 group. (I) KEGG pathway enrichment analysis of DEGs in the M2 vs. M3 group. (J) KEGG pathway enrichment analysis of DEGs in the F1 vs. M1 group. (K) KEGG pathway enrichment analysis of DEGs in the F2 vs. M2 group. (L) KEGG pathway enrichment analysis of DEGs in the F3 vs. M3 group. The top 20 metabolic pathways significantly enriched for DEGs in different subgroups are shown. Triangles represent up-regulated genes, inverted triangles represent down-regulated genes, and circles represent genes that are both up-regulated and down-regulated, and the size of these three images represents the number of DEGs in the pathway. Colors represent significance.

Functional analysis of DEGs

GO and KEGG enrichment analyses were performed on the DEGs produced during different flower stages of *S. variegata* in both male and female flowers, and the results of GO analyses showed that the DEGs produced during the three developmental stages of *S. variegata* in both male and female flowers were mainly enriched in the areas of biological processes, cellular components, and molecular functions. Among them, female flowers were significantly enriched in detoxification, rhythmic process, transporter activity, and transcription regulator activity; male flowers were mainly enriched in detoxification, transporter activity, and transcription regulator activity (Supplementary Fig. S1C-E). 126, 114 and 113 pathways were enriched in the F1 vs. F2, F1 vs. F3 and F2 vs. F3 comparison groups of female flowers, respectively. F1 vs. F2 was significantly enriched in pathways such as Plant hormone signal transduction (ko04075), Photosynthesis (ko00195), ABC transporters (ko02010), Carbon fixation in photosynthetic organisms (ko00710), Fatty acid elongation (ko00062), and Pentose phosphate pathway (ko00030). F1 vs. F3 was significantly enriched in pathways such as Plant hormone signal transduction, Pentose phosphate pathway, Carbon metabolism (ko01200), Photosynthesis, Carbon fixation in photosynthetic

organisms, and ABC transporters. F2 vs. F3 was significantly enriched in pathways such as Plant–pathogen interaction (ko04626), Fatty acid elongation, Starch and sucrose metabolism (ko00500), Glycerolipid metabolism (ko00561), and Steroid biosynthesis (ko00100). 133, 135 and 108 pathways were enriched in the M1 vs. M2, M1 vs. M3, and M2 vs. M3 comparison groups of male flowers, respectively. M1 vs. M2 was significantly enriched in pathways such as Plant hormone signal transduction, Flavonoid biosynthesis (ko00941), other glycan degradation (ko00511), ABC transporters, Valine, leucine, and isoleucine degradation (ko00280), and Fatty acid elongation. M1 vs. M3 was significantly enriched in pathways such as Plant–pathogen interaction, Plant hormone signal transduction, MAPK signaling pathway–plant (ko04016), Glutathione metabolism (ko00480), Flavonoid biosynthesis, and beta–Alanine metabolism (ko00410). M2 vs. M3 was significantly enriched in pathways such as Plant hormone signal transduction, Cutin, suberine and wax biosynthesis (ko00073), Glycerolipid metabolism, ABC transporters, and Pentose and glucuronate interconversions (ko00040). 75, 133 and 126 pathways were enriched in the F1 vs. M1, F2 vs. M2, F3 vs. M3, respectively. F1 vs. M1 was significantly enriched in pathways such as Plant–pathogen interaction, Plant hormone signal transduction, Starch and sucrose metabolism, MAPK signaling pathway – plant, alpha-Linolenic acid metabolism (ko00592), and Linoleic acid metabolism (ko00591). F2 vs. M2 was significantly enriched in pathways such as Fatty acid elongation, Glycerolipid metabolism, Starch and sucrose metabolism, Carbon metabolism, and Photosynthesis – antenna proteins. F3 vs. M3 was significantly enriched in pathways such as Phenylpropanoid biosynthesis, Flavonoid biosynthesis, Benzoxazinoid biosynthesis (ko00402), Plant hormone signal transduction, and Photosynthesis – antenna proteins (ko00196) (Fig. 1D–L). Although there were differences in the pathways of DEG enrichment between male and female flowers at different developmental stages, it is still evident that DEGs are mainly involved in the synthesis of flavonoids and amino acids, among others, as male and female flowers develop.

Cluster analysis of DEGs

We obtained the expression trends of 12,245 DEGs during the development of male and female flowers of *S. variegata* by K-means clustering analysis. All DEGs co-clustered into 18 clusters in female flowers and 17 clusters in male flowers (Fig. 2, Supplementary Fig. S2). Similar expression trends were clustered into the same clusters in testing the potential role of DEGs, high expression in F3 and F2 (e.g., Cluster 2, cluster 3, cluster 5, cluster 6, and cluster 13) had Phenylpropanoid biosynthesis (ko00940), Nitrogen metabolism (ko00910), Galactose metabolism (ko00052), Flavonoid biosynthesis, Steroid biosynthesis, and Photosynthesis. Highly expressed in F1 (e.g., cluster7, cluster9, cluster10, cluster14, cluster15, and cluster17) were Plant hormone signal transduction, Glycolysis / Gluconeogenesis (ko00010), Flavonoid biosynthesis, Glycerolipid metabolism, Betalain biosynthesis (ko00965), Plant–pathogen interaction, and Phosphatidylinositol signaling system (ko04070). Highly expressed in M3 (e.g., cluster1, cluster4, cluster8, cluster9, and cluster15) were Phenylpropanoid biosynthesis, Plant hormone signal transduction, Glycerolipid metabolism, and Plant–pathogen interaction. Highly expressed in M2 (cluster3, cluster5, cluster7, cluster11, cluster12, and cluster17) were Pentose and glucuronate interconversions, Flavonoid biosynthesis, Phenylpropanoid biosynthesis, Nitrogen metabolism (ko00910), Glucosinolate biosynthesis (ko00966), and Carotenoid biosynthesis (ko00906). Highly expressed in M1 (e.g., cluster2, cluster6, cluster10, cluster14, and cluster15) were DNA replication (ko03030), Plant hormone signal transduction, Starch and sucrose metabolism, Linoleic acid metabolism, and Glycerolipid metabolism. K-means clustering analysis of DEGs from different periods of male and female flowers yielded results similar to the functional analysis of DEGs, which mainly regulated the biosynthesis of flavonoids, phenylpropanoids, and a variety of amino acids during the development of male and female flowers, suggesting that the biosynthesis of these substances is a key pathway in the development of male and female flowers of *S. variegata*.

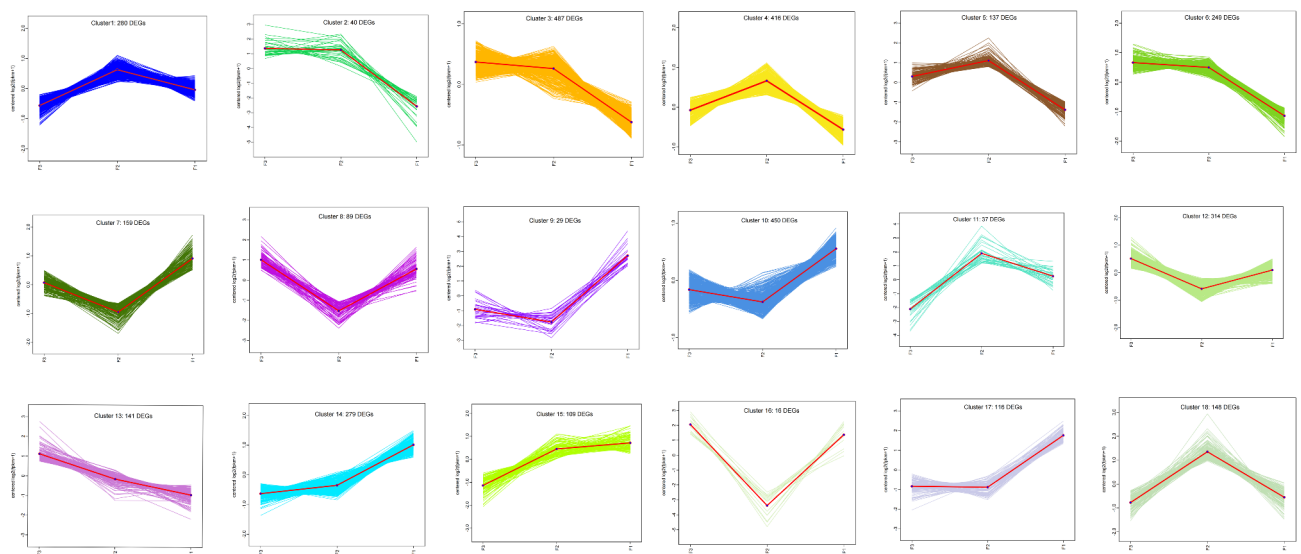


Fig. 2. K-Means clustering analysis of DEGs for three developmental periods of *S. variegata* female flowers.

Transcription factor analysis

To understand the underlying molecular mechanisms of male and female flower development in *S. variegata*, highly expressed TFs were further identified and analyzed. Interestingly, we found a large number of TFs in different flowering periods of *S. variegata* male and female flowers. Among them, *RLK*, *ERF*, *MYB*, *bHLH*, *C2H2*, *MIKC_MADS*, and *NAC* TFs were expressed in different flowering periods of male and female flowers (Supplementary Fig. S3). Overall, TFs were more highly expressed at all stages of male than female flowers and more DEGs were down-regulated than up-regulated at different times in both male and female flowers. Among the predicted gene families, *RLK*, *C2H2*, and *WRKY* were significantly up-regulated in F2 and F3 of female flowers, and *ERF*, *MYB*, *bZIP*, and *TALE* were significantly down-regulated in F2 and F3 of female flowers. *RLK*, *NAC*, and *WRKY* were significantly up-regulated in M2 and M3 of male flowers, and *MYB*, *bHLH*, *C2H2*, and *MIKC_MADS* were significantly down-regulated in M2 and M3 of male flower. *ERF*, *MYB*, and *bHLH* were significantly down-regulated and *RLK*, *MIKC* were significantly up-regulated in M2 compared to F2. Compared with F3, *RLK*, *bHLH*, *ERF*, and *C2H2* were significantly down-regulated and *NAC*, *WRKY*, *MIKC* were significantly up-regulated in M3 (Supplementary Table S3).

Statistical analysis of metabolites

A total of 5,855 metabolites were detected and quantified by LC-MS/MS, containing compounds such as organic acids and their derivatives, organic heterocyclic compounds, lipids, benzoic acids, phenylpropanoids, and polyketides. Among them, more substances were fatty acids, terpene glycans, diterpenes, linolenic acid, and its derivatives, etc. The results of PCA analyses showed that the metabolites of different periods of male and female flowers were differentiated. The metabolites of F3 and M3 could be clearly distinguished from the other periods of male and female flowers, suggesting that the end of the female flower and the end of the male flower were the most different (Supplementary Fig. S4A). The accumulation characteristics of metabolites in *S. variegata* female and male flowers at different developmental stages could be analyzed by clustering heat maps, and the results showed that there were significant differences in metabolites between male and female flowers as well as at different developmental stages of the same type of flower (Supplementary Fig. S4B). The metabolites were categorized into four clusters in total, with the metabolites in cluster 1 being the most abundant in F2 and the least abundant in M3. Metabolites in cluster 2 were most abundant in F3 and least abundant in M3. Metabolites in cluster 3 were most abundant in M3 and least abundant in M1. Metabolites in cluster 4 were most abundant in M1 and least abundant in F2. From both principal component analysis and cluster heat map analysis, it can be concluded that the metabolites of *S. variegata* female and male flowers changed significantly in different developmental stages.

DEMs function analysis

A total of 4,145 DEMs were screened based on the orthogonal projections to latent structures- discriminant analysis (OPLS-DA) model combined with variable importance in projection (VIP) ≥ 1 , FC ≥ 1 , and P-value ≤ 0.01 (Supplementary Table S4). Among the female flowers, the F2 vs. F3 comparison group had the most DEMs (1,509), of which 842 metabolites were up-regulated and 667 metabolites were down-regulated. Among male flowers, the M1 vs. M3 comparison group had the highest number of DEMs (2,194), of which 1,324 metabolites were up-regulated and 870 metabolites were down-regulated. The most DEMs were accumulated in F3 vs. M3 and the least in F1 vs. M3 during the same flowering period in female and male flowers. There was a significant increase in the content of 1,014 DEMs and a substantial decrease in the content of 690 DEMs in M3 compared to F3. The number and accumulation of DEMs increased gradually with the opening of both male and female flowers (Supplementary Fig. S4C-K).

KEGG enrichment analysis between different comparison groups of female and male flowers showed that 87, 81, and 102 metabolic pathways were annotated in the three comparison groups of female flowers, respectively. 11, 5, and 8 of these pathways were significantly enriched, respectively. The three comparison groups of male flowers were annotated to 98, 99, and 102 metabolic pathways, respectively. 4, 9, and 7 of these pathways were significantly enriched, respectively. The three comparison groups of female and male flowers of the same flowering stage were annotated to 71, 95, and 98 metabolic pathways. Nicotinate and nicotinamide metabolism (ko00760), Arginine biosynthesis (ko00220), Alanine, aspartate, and glutamate metabolism (ko00250), and Phenylalanine, tyrosine and tryptophan biosynthesis (ko00400) metabolic pathways were significantly enriched in F1 vs. F2. Phenylpropanoid biosynthesis, Betalain biosynthesis (ko00965), Glucosinolate biosynthesis (ko00966), Pyrimidine metabolism (ko00240), and Vitamin B6 metabolism (ko00750) metabolic pathways were significantly enriched in F1 vs. F3. Phenylpropanoid biosynthesis, Carbon fixation in photosynthetic organisms, Alanine, aspartate and glutamate metabolism, Pentose and glucuronate interconversions, and Pyruvate metabolism (ko00620) metabolic pathways were significantly enriched in F2 vs. F3. Pyruvate metabolism, Aflatoxin biosynthesis (ko00254), Flavonoid biosynthesis, and Phosphatidylinositol signaling system (ko04070) metabolic pathways were significantly enriched in M1 vs. M2. Phenylpropanoid biosynthesis, Monoterpenoid biosynthesis, Neomycin, kanamycin, and gentamicin biosynthesis, Phenylalanine metabolism, and Tyrosine metabolism (ko00350) metabolic pathways were significantly enriched in M1 vs. M3. Vitamin B6 metabolism, Pentose and glucuronate interconversions, Nicotinate and nicotinamide metabolism, Glyoxylate and dicarboxylate metabolism (ko00630), and Nitrogen metabolism metabolic pathways were significantly enriched in M2 vs. M3. Phenylalanine, tyrosine and tryptophan biosynthesis, Pentose and glucuronate interconversions, Glyoxylate and dicarboxylate metabolism, and Fatty acid elongation (ko00062) metabolic pathways were significantly enriched in F1 vs. M1. Flavone and flavonol biosynthesis, Isoflavonoid biosynthesis (ko00943), Phenylpropanoid biosynthesis, and Flavonoid biosynthesis metabolic pathways were significantly enriched in F2 vs. M2. Flavone and flavonol biosynthesis, Monoterpenoid biosynthesis (ko00902), and Alanine, aspartate and glutamate metabolism (ko00250) metabolic pathways were significantly enriched in F3 vs. M3. Among them,

Phenylpropanoid biosynthesis and Flavonoid biosynthesis were more enriched at the full and final bloom stages (Fig. 3).

Transcriptome and metabolome in combination analysis

Common metabolic pathways were obtained by comparing the metabolic pathways involved in DEGs vs. DEMs. The results of the Venn diagram showed that there were 79, 70, and 84 common metabolic pathways between DEGs and DEMs in F1 vs. F2, F1 vs. F3, and F2 vs. F3, respectively. There were 92, 95, and 80 common metabolic pathways between DEGs and DEMs in M1 vs. M2, M1 vs. M3, and M2 vs. M3, respectively. There were 35, 90, and 89 common metabolic pathways between DEGs and DEMs in F1 vs. M1, F2 vs. M2, F3 vs. M3 (Fig. 4A–I). We selected the 30 pathways with the most significant enrichment of common pathways in each subgroup for enrichment analysis. The results showed that Phenylpropanoid biosynthesis, Pentose and glucuronate interconversions, and Flavonoid biosynthesis pathways were the most significant metabolic pathways during the development of male and female flowers of *S. variegata* (Fig. 4J–R).

To elucidate the relevance of DEGs and DEMs related to phenylpropanoids, flavonoids, etc., we constructed the integration pathways for the three developmental stages of male and female flowers of *S. variegata* (Fig. 5A). In the biosynthesis pathway of phenylpropanoid and flavonoids, the expression of 4-coumarate-CoA ligase (4CL: Sva01G002770, Sva01G004170, Sva03G006690, Sva03G014220, Sva06G013710, Sva10G004990, Sva12G008250, Sva12G008260, Sva15G009870, Sva17G002660, Sva17G012550), Cinnamyl-alcohol dehydrogenase (CAD: Sva09G007840, Sva16G017940), Ferulate-5-hydroxylase (F5H: Sva05G008980, Sva07G001420), and Catechol-O-Methyltransferase (COMT: Sva12G000240, Sva12G000580, Sva14G007990, Sva14G008010, Sva16G028990, Sva16G029010) was F3 > F2 > F1, M3 > M2 > M1, and with the development of male and female flowers, the high expression of these genes promoted the accumulation of Ferulic acid, Sinapic acid, 5-Hydroxyconiferinaldehyde, Sinapoyl-CoA, and Sinapyl alcohol accumulation, which ultimately promoted the synthesis of large amounts of Syringin. The expression of Anthocyanidin synthase (ANS: Sva01G009400, Sva03G008470, Sva06G008290,

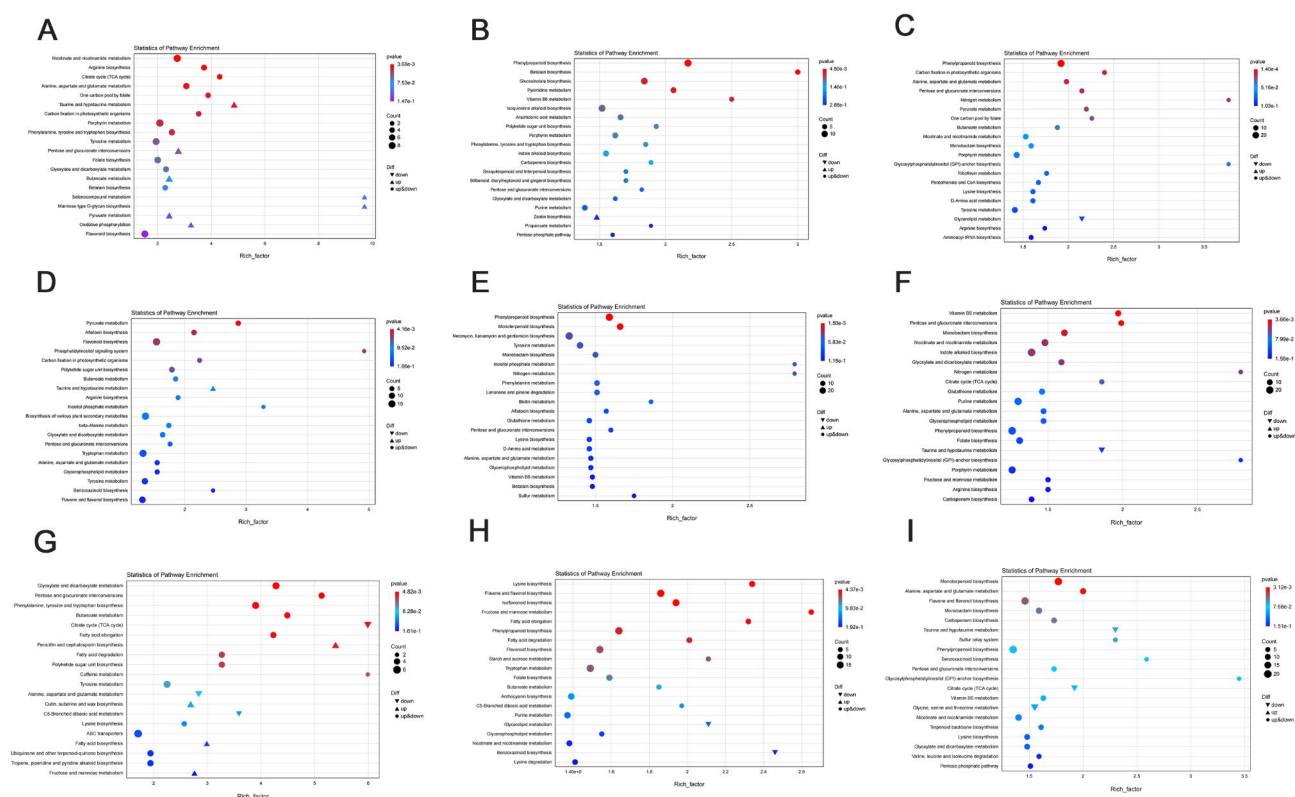


Fig. 3. KEGG metabolic pathway enrichment analysis of DEMs between different groupings of *S. variegata* male and female flowers (A) KEGG metabolic pathway enrichment of DEMs in F1 vs. F2. (B) KEGG metabolic pathway enrichment of DEMs in F1 vs. F3. (C) KEGG metabolic pathway enrichment of DEMs in the F2 vs. F3. (D) KEGG metabolic pathway enrichment of DEMs in the M1 vs. M2. (E) KEGG metabolic pathway enrichment of DEMs in the M1 vs. M3. (F) KEGG metabolic pathway enrichment of DEMs in the M2 vs. M3. (G) KEGG metabolic pathway enrichment of DEMs in the F1 vs. M1. (H) KEGG metabolic pathway enrichment of DEMs in the F2 vs. M2. (I) KEGG metabolic pathway enrichment of DEMs in the F3 vs. M3. The top 20 metabolic pathways significantly enriched in DEGs in different subgroups are shown. Triangles represent up-regulated genes, inverted triangles represent down-regulated genes, and circles represent both up- and down-regulated genes, and the size of these three images represents the number of DEGs in the pathway. Colors represent significance.

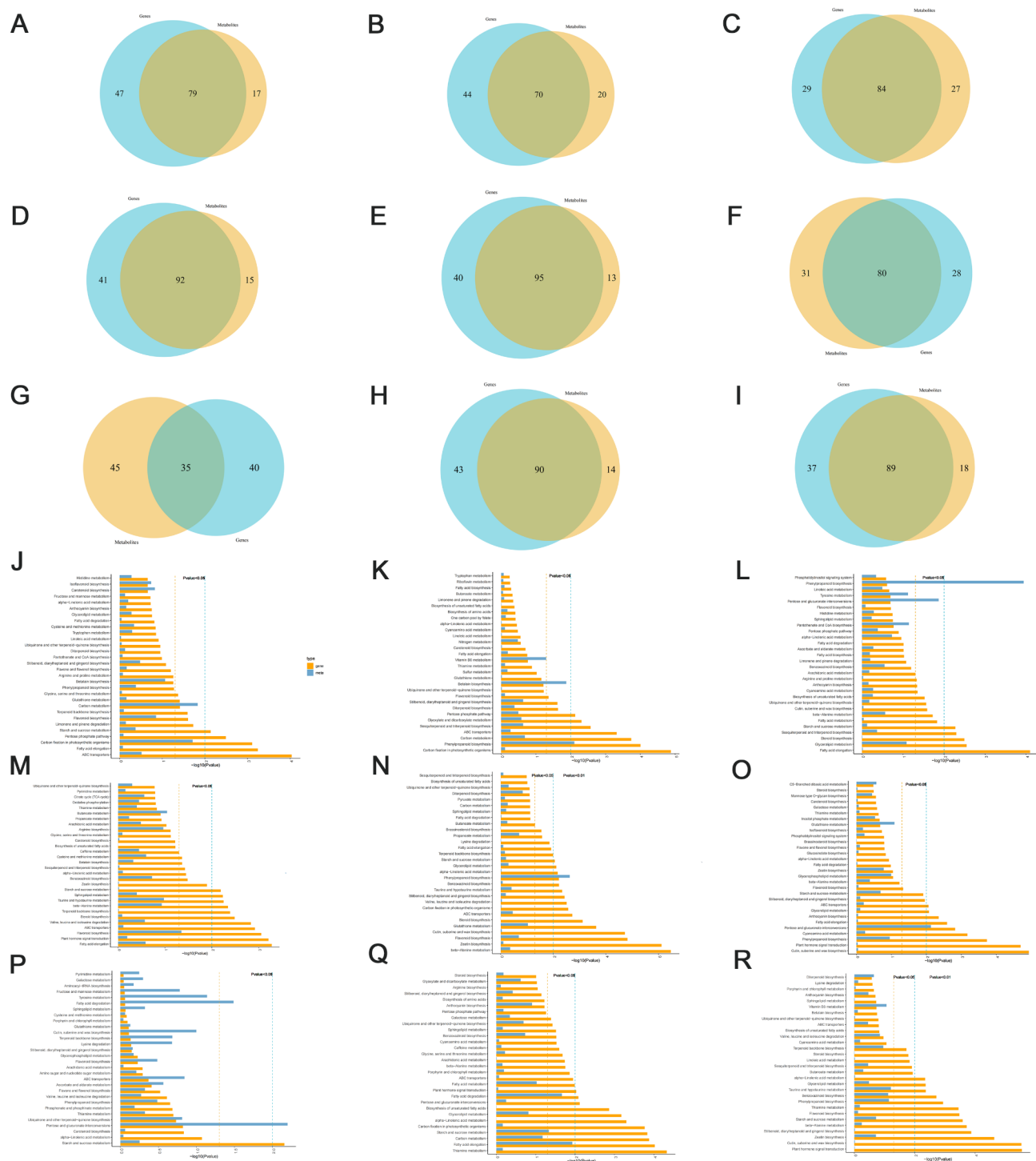


Fig. 4. Analysis of common pathways of transcriptome and metabolome at different developmental stages of *S. variegata* male and female flowers (A) Venn diagram of the pathways of DEGs and DEMs in the F1 vs. F2. (B) Venn diagram of the pathways of DEGs and DEMs in the F1 vs. F3. (C) Venn diagram of the pathways of DEGs and DEMs in the F2 vs. F3. (D) Venn diagram of the pathways of DEGs and DEMs in the M1 vs. M2. (E) Venn diagram of the pathways of DEGs and DEMs in the M1 vs. M3. (F) Venn diagram of the pathways of DEGs and DEMs in the M2 vs. M3. (G) Venn diagram of the pathways of DEGs and DEMs in the F1 vs. M1. (H) Venn diagram of the pathways of DEGs and DEMs in the F2 vs. M2. (I) Venn diagram of the pathways of DEGs and DEMs in the F3 vs. M3. (J) Co-enrichment pathway analysis of DEGs and DEMs in F1 vs. F2. (K) Co-enrichment pathway analysis of DEGs and DEMs in F1 vs. F3. (L) Co-enrichment pathway analysis of DEGs and DEMs in F2 vs. F3. (M) Co-enrichment pathway analysis of DEGs and DEMs in the M1 vs. M2. (N) Co-enrichment pathway analysis of DEGs and DEMs in the M1 vs. M3. (O) Co-enrichment pathway analysis of DEGs and DEMs in the M2 vs. M3. (P) Co-enrichment pathway analysis of DEGs and DEMs in the F1 vs. M1. (Q) Co-enrichment pathway analysis of DEGs and DEMs in the F2 vs. M2. (R) Co-enrichment pathway analysis of DEGs and DEMs in the F3 vs. M3.

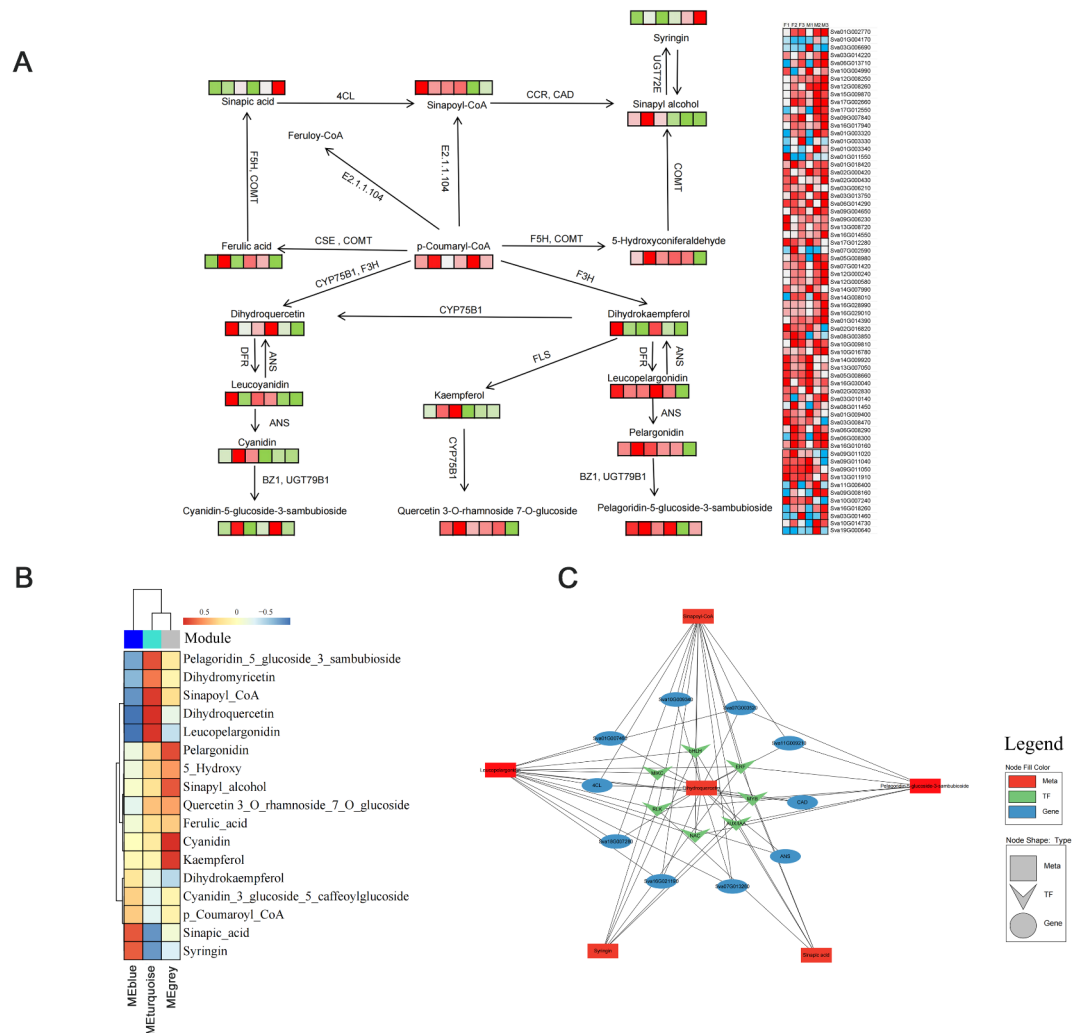


Fig. 5. Joint analysis of DEGs and DEMs involved in different developmental stages of male and female flowers of *S. variegata* (A) Integration pathways of DEGs and DEMs involved in phenylpropanoid and flavonoid biosynthesis. Pathways were remapped according to ko00940, ko00941, ko00942, ko00944, ko00945 in the KEGG database (www.kegg.jp/kegg/kegg1.html). The Kanehisa laboratory have happily provided permission). Red and green colors indicate metabolites with relatively high levels and metabolites with relatively low levels, respectively. Red and blue colors indicate genes with up-regulated expression and genes with down-regulated expression, respectively. From left to right, the six squares represent the three extremes of *S. variegata* male and female flower. COMT (Sva12G000240, Sva12G000580, Sva14G007990, Sva14G008010, Sva16G028990, Sva16G029010). CSE, *caffeoylshikimate esterase* (Sva01G014390, Sva02G016820, Sva08G003850, Sva10G009810, Sva10G016780, Sva14G009920, Sva13G007050). 4CL (Sva01G002770, Sva01G004170, Sva03G006690, Sva03G014220, Sva06G013710, Sva10G004990, Sva12G008250, Sva12G008260, Sva15G009870, Sva17G002660, Sva17G012550). F5H (Sva05G008980, Sva07G001420). CCR, *cinnamoyl-CoA reductase* (Sva01G003320, Sva01G003330, Sva01G003340, Sva01G011550, Sva01G018420, Sva02G000420, Sva02G000430, Sva03G006210, Sva03G013750, Sva06G014290, Sva09G004650, Sva09G006230, Sva13G008720, Sva16G014550, Sva17G012280). CAD (Sva09G007840, Sva16G017940). UGT72E, *coniferyl-alcohol glucosyltransferase* (Sva07G002590). E2.1.1.104, *caffeoyl-CoA O-methyltransferase* (Sva09G008160, Sva10G007240, Sva16G018260). F3H, *naringenin 3-dioxygenase* (Sva05G008660, Sva16G030040). CYP75B1, *flavonoid 3'-monooxygenase* (Sva13G007050). DFR, (Sva02G002830, Sva03G010140, Sva08G011450). ANS (Sva01G009400, Sva03G008470, Sva06G008290, Sva06G008300, Sva16G010160). FLS (Sva03G001460, Sva10G014730, Sva19G000640). BZ1 (Sva09G011020, Sva09G011040, Sva09G011050, Sva13G011910). UGT79B1 (Sva11G006400). (B) Correlation heat map of gene expression of each module and important DEMs in *S. variegata*. (C) Network of relationships between TFs, DEGs, and metabolites involved in the phenylpropanoid and flavonoid pathways. The green, pink, and rose node sub-tables represent key genes, key TFs, and key metabolites related to *S. variegata* flower development.

Sva06G008300, Sva16G010160), *Anthocyanidin 3-O-glucosyltransferase* (BZ1: Sva09G011020, Sva09G011040, Sva09G011050, Sva13G011910), *Flavonol synthase* (FLS: Sva03G001460, Sva10G014730, Sva19G000640), and *Anthocyanidin 3-O-glucoside 2^{''}-O-xylosyltransferase* (UGT79B1: Sva11G006400) was highest at the full bloom stage of both male and female flowers, and *Bifunctional dihydroflavonol 4-reductase* (DFR) subsequently converted the two main substrates (dihydrokaempferol, dihydroquercetin) into Leucopelargonidin and Leucopelargonidin. With the development of both male and female flowers of *S. variegata*, the expression of *ANS*, *DFR*, and *BZ1* genes were gradually down-regulated for expression at subsequent developmental stages, whereas the increased expression of *FLS* promoted the synthesis of Kaempferol, which ultimately synthesized large amounts of Cyanidin-5-glucoside-3-sambubioside, Pelagoridin-5-glucoside-3-sambubioside, and Quercetin 3-O-rhamnoside 7-O-glucoside. Some of the metabolites were consistent with their upstream gene expression, such as Sinapic acid, Syringin, and Cyanidin-5-glucoside-3-sambubioside. It can be seen that during the development of male and female flowers of *S. variegata*, the content of phenylpropanoids and flavonoids gradually increased with the development of flowers.

We further utilized 12,245 genes and 17 important DEMs related to synthesizing phenylpropanoids and flavonoids as source data for a weighted gene co-expression network module for analysis (WGCNA). Three modules- blue, turquoise, and grey- were identified in the cluster tree. The results of the relationship between the gene modules and the significant DEMs indicated that the blue and turquoise modules had a higher correlation with them. Genes in the blue module were significantly positively associated with Syringin and Sinapic_acid, and significantly negatively associated with Pelagoridin_5_glucoside_3_sambubioside, Dihydromyricetin, Sinapoyl-CoA, and Leucopelargonidin were significantly negatively correlated. Genes in the turquoise module were associated with Pelagoridin_5_glucoside_3_sambubioside, Dihydromyricetin, Sinapoyl-CoA, Dihydroquercetin, and Leucopelargonidin significantly positively and significantly negatively associated with Syringin and Sinapic_acid (Fig. 5B). 40 hub genes were screened based on correlation coefficients between candidate genes in the blue and turquoise modules, where correlation coefficients $r > 0.8$, and P-values < 0.05 . Hub genes, high-expression TFs, and 17 significant DEMs were utilized to construct networks of interactions between them. 10 key genes (*4CL*: Sva01G002770, *ANS*: Sva06G008300, *CAD*: Sva09G007840, *gibberellin 3beta-dioxygenase* (*GA3ox*): Sva18G007280, *RPM1-interacting protein 4* (*RIN4*): Sva16G021190, *mitogen-activated protein kinase kinase kinase 2* (*MAP3K2*): Sva07G003520, *peptide-methionine (R)-S-oxide reductase* (*msrB*): Sva11G009210, *glutathione peroxidase* (*GPX*): Sva07G013260, *tuliposide A-converting enzyme* (*TCEA*): Sva10G009340, *E3 ubiquitin-protein ligase RNF38/44* (*RNF38_44*): Sva01G007460), 7 TFs (*AUX/IAA*, *bHLH*, *MYB*, *NAC*, *ERF*, and *RLK*), and 6 key metabolites (Syringin, Sinapic acid, Sinapoyl-CoA, Dihydroquercetin, Pelagoridin-5-glucoside-3-sambubioside, and Leucopelargonidin) were selected. Among these, *4CL* and *ANS* were positively correlated with Syringin and negatively correlated with Dihydrokaempferol, Sinapic acid, and Leucopelargonidin. *GA3ox*, *RIN4*, *MAP3K2*, *msrB*, *GPX*, *TCEA*, *RNF38_44*, *UX/IAA*, *bHLH*, *MYB*, *NAC*, *ERF*, and *RLK* were negatively correlated with Syringin, Sinapic acid, Sinapoyl-CoA, Dihydroquercetin, Pelagoridin-5-glucoside-3-sambubioside, and Leucopelargonidin (Fig. 5C). The results suggest that TFs and key genes may mediate the metabolism of phenylpropanoid and flavonoids, which further regulate flower development in *S. variegata*.

DEGs validation by qRT-PCR

To check the accuracy of the differentially expressed genes, the expression of 19 representative DEGs was examined using quantitative real-time PCR (qRT-PCR) at three flowering stages of both male and female flowers of the *S. variegata* (Fig. 6, Supplementary Table S5). The DEGs were associated with phenylpropanoid and flavonoid biosynthesis in flower development. The relative expression levels of qRT-PCR and RNA-seq were logarithmized between different flowering stages. Correlation analysis was performed using the above logarithmic results, and the expression patterns were consistent with the RNA-seq data.

Discussion

S. variegata, as a perennial shrub of the *Salix* genus, is a typical dioecious plant with good flooding, drought, and heavy metal pollution resistance, making it an excellent ecological restoration plant²⁸. It grows mainly in the riparian zone and experiences the effects of water level subsidence in the riparian zone all year round. The flowering period of *S. variegata* is generally June- December, which overlaps with the time of flooding. However, it was found that *S. variegata* has a large number of seeds and its viability is unaffected. The molecular regulatory mechanisms of its floral ontogeny and development are worthy of our attention. In the last 30 years, many processes in flower development have been understood in detail through genetic and molecular analyses, and despite significant progress, many questions about the regulation of flower development in angiosperms remain unanswered²⁹. In angiosperms, flowering is a trait of the plant that adapts to its environment and is important for its survival and reproduction³⁰. The occurrence and development of floral organs is a complex process³¹. The complex flowering mechanism is not only regulated by many highly conserved genes but also influenced by external environmental factors such as photoperiod, temperature, and humidity³². Therefore, the data of a single omics cannot fully analyze the process of macro-development, and the multi-omics integration verification can make up for the missing data of a single omics analysis and reduce the false positives caused by a single omics analysis. In this study, we used the method of transcriptome and metabolome joint analysis to explore the regulation mechanism of *S. variegata* male and female flower development.

We obtained a total of 12,245 DEGs by transcriptomic analysis, 20 DEGs shared among the three developmental stages of female flowers, F1 vs. F2, F1 vs. F3 and F2 vs. F3 with 1,281, 374, and 650 specifically expressed DEGs, respectively, and 383 DEGs shared among the three periods of male flowers, M1 vs. M2, M1 vs. M3 and M2 vs. M3 had 2,208, 1,680 and 81 specifically expressed DEGs, respectively. 54 DEGs shared

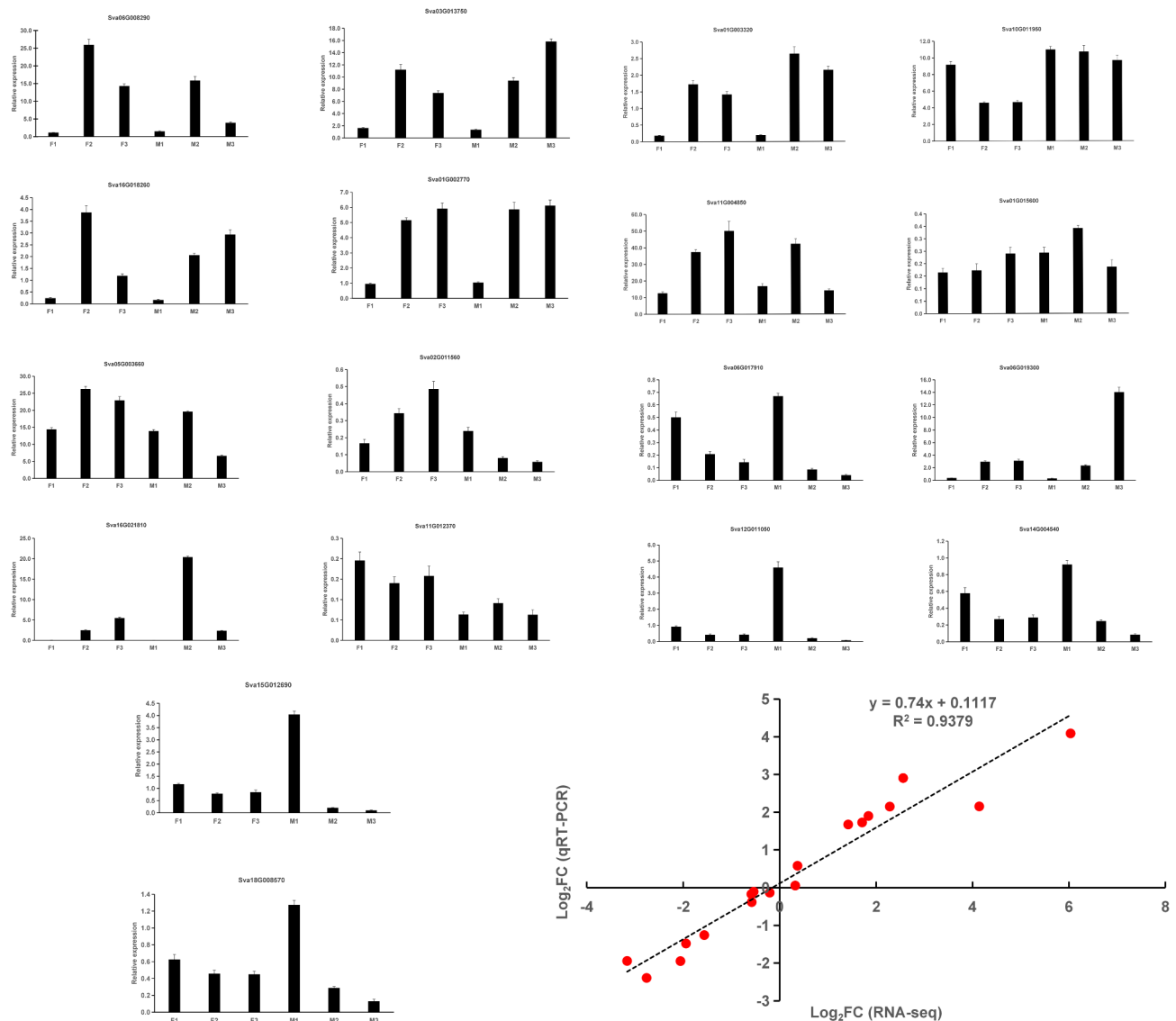


Fig. 6. Validation of the expression of genes related to the development of male and female flowers in *S. variegata*. The expression levels of 18 flower development-related genes were verified at three floral stages in male and female flowers using qRT-PCR. The relative expression levels of 18 DEGs were calculated using the $2^{-\Delta\Delta C_t}$ method; *TIP41* (Sva09G007630) served as an internal reference gene.

among the three comparison groups of male and female flowers at the same flowering stage, and 292, 3,646, and 1,300 specifically expressed DEGs in F1 vs. M1, F2 vs. M2, and F3 vs. M3, respectively. The highest number of DEGs were screened from bud to full bloom stage in both female and male flowers, suggesting the need for more genes to be involved in the *S. variegata* bud-to-flowering process. TFs play an important role in plant growth and development, not only can they be directly induced by signals related to life activities, but also through interactions with other proteins or direct regulation of the expression of downstream target genes, thus participating in the complex network of signaling and regulation corresponding to the growth and development of plants³³. In this study, we identified and analyzed the highly expressed TFs during the development of male and female flowers of *S. variegata*, and found a large number of differentially expressed TFs, among which *AUX/IAA*, *bHLH*, *MYB*, *ERF*, and *RLK* gene families were more highly expressed, which are involved in the differentiation of male and female flowers of *S. variegata*. The *MADS-box* gene family is involved in various stages of plant development, mainly promoting plant nutrient growth, determining the characteristics of floral organs, regulating the timing of flowering, promoting the formation of pollen and embryo sacs, and regulating the development of seeds and fruits^{34,35}. The *mads-box* gene family is divided into two types: type I (*M_Type*) and type II (*MIKC*), which were originally identified as floral organ signature genes in *Arabidopsis thaliana* and *Antirrhinum majus*³⁶. In this study, *MIKC* genes have important regulatory roles in the development of male and female flowers in *S. variegata*, with significant up- and down-regulation at different developmental periods. Previous studies have shown that *MIKC-type* genes play a more important role in plant floral organ development³⁷. In contrast, we similarly found a portion of the *MIKC* gene significantly up-regulated in both

male and female flowers of *S. variegata* at the bud stage, and the full bloom stage and the final bloom stage reduced its expression. Auxin is an important hormone in the development process of plant flowers, which can affect the development of inflorescence and flower organs³⁸. Auxin signaling consists of four core components: *AUX/IAA*, *AUX/LAX*, transport inhibitor response 1/auxin signaling F-box protein (*TIR1/AFB*), and ARF family member proteins³⁹. It has been shown that members of the *MYB* gene family are key players in the late stages of floral organ development and maturation, involved in nectar development, stamen development, pistil length, secondary metabolites such as flavonols, phenylpropanoids, and odor compounds^{40–43}. *ERF* is one of the largest families of TFs in plants, and it plays a key role in transcriptional regulation during flower senescence⁴⁴. It has been shown that TFs such as *NAC* are associated with senescence in several tissues of *Arabidopsis thaliana*, including petals and angiosperms⁴⁵. The *NAC* family is the second largest family of transcription factors in plants, and *NAC* are involved in the regulation of a variety of processes such as flower development and growth hormone signaling⁴⁶. *NAC* have strong activity during flower development, which also reflects that they may be one of the important regulators of male and female flower development in *S. variegata*. The *bHLH* TF family regulates *CONSTANS* in *Arabidopsis*, which is essential for photoperiodic flowering. In this study, a large number of *bHLH* genes were identified, which were highly expressed during different developmental periods of male and female flowers of *S. variegata* and may play an essential role in the regulation of the development of male and female flowers of *S. variegata*^{47–49}. *RLK* belongs to a large subfamily of proteins that can transmit ligand signals through autophosphorylation and initiate signaling cascades⁵⁰. The *RLK* is involved in plant flower development, especially in pollen germination and pollen tube growth^{51,52}. In this study, the *RLK* genes were the most abundant and, as in previous studies, this class of transcription factors was highly expressed in male flowers of *S. variegata*, and some of the *RLKs* were significantly up-regulated for expression during the bud and full bloom stage in both male and female flowers⁵³.

Flower development is a process of floral transition from autotrophic to heterotrophic, during which floral secondary metabolism immediately^{49,54}. As expected, the process of pathways involved in secondary metabolite synthesis was significantly enriched. At this time, metabolite accumulation is related to traits such as color and smell, and these changes depend on the pollinators, precursors, etc⁵⁵. Plants are able to synthesize a range of phenylpropanes and flavonoids that are important in plant growth, development, flowering, and pigmentation⁵⁶. Anthocyanins are associated with flower color formation, and flavonoids and phenylpropanoid compounds are co-pigments that stabilize anthocyanins, and both metabolites are synthesized via the phenylpropane-related pathway⁵⁷. It has been demonstrated that flavonoids and phenylpropanoid-related genes are highly expressed during the flowering stage of plants⁵⁸. In our study, the stigma of female flowers of *S. variegata* slowly changes from golden yellow to brown after flowering, and the anthers of male flowers are also golden yellow and gradually turn brown, which may also be caused by the gradual accumulation of phenylpropanoid and flavonoids and their derivatives. Similarly, flavonoids and phenylpropanoid-related genes were significantly higher in expression during the full bloom stage and the final bloom stage in both female and male flowers of *S. variegata*. Consistent with the changes in gene expression, the flavonoid and phenylpropane biosynthetic pathways were also enriched from the flower bud stage to the final flowering stage. To attract pollinators during flowering, plants often produce volatiles and pigments, including phenylpropanoids and flavonoids. The increased accumulation of these two types of substances during the development of male and female flowers of *S. variegata* may also serve to attract insect pollinators. These results are similar to previous studies on flower development in *Lonicera japonica* Thunb, *Rosmarinus officinalis* L., and *Pogostemon cablin* (Blanco) Benth., among others^{32,58,59}. It has been shown that the synthesis of flavonoids often requires the production of precursors via the phenylpropane pathway, and these processes involve many important enzymes such as *4CL*, *ANS*, *F5H*^{60,61}. Some studies have found that some related genes regulating plant hormones, such as GA signaling-related genes and growth hormone signaling-related genes, are negatively correlated with flavonoids and phenylpropanoids. In this study, we found that phytohormone-related signaling pathways were also enriched during the development of male and female flowers of *S. variegata*, suggesting that GA and growth hormone signaling may be involved in the metabolism and biosynthesis of flavonoids, phenylpropanoids, and their derivatives⁶². *GA3ox* is a target gene for GA biosynthesis, which can affect stamen development. Consistent with previous studies, the gene *GA3ox* was significantly up-regulated in male and female flowers during the development of male and female flowers in *S. variegata*. Many studies have shown that *MAP3K*, *RIN4*, regulates various physiological and biochemical processes throughout the plant growth cycle, including germ cell and embryo development, flower development^{63,64}. The *msrB* is an active enzyme in plants that is more abundant in plant developing organs⁶⁵. *TCEA*, *RNF38_44* are also active substances in plants that influences growth and development and enhances resistance in plants^{66,67}. The *GPX* plays a crucial role in inducing oxidative stress and promoting plant cell growth⁶⁸. Functional clustering of these genes, which we found to be significantly up-regulated and mostly associated with flavonoid and phenylpropanoid synthesis during the developmental stages of both male and female flowers of *S. variegata*, further highlighted the key biological processes and molecular functions related to flavonoid production. In addition, KEGG enrichment analysis revealed that these genes were associated with flavonoid and phenylpropanoid metabolism. Through combined transcriptomic and metabolomic analyses, we found that TFs could regulate the biosynthesis of flavonoids and phenylpropanes by regulating their biosynthesis-related genes. The changes of DEMs and DEGs in these pathways were similar during the different developmental periods of *S. variegata* male and female flowers. *S. variegata* in both male and female flowers were similar in terms of their trends in different developmental periods. This suggests that the above genes play an important role in regulating the accumulation of this metabolite in *S. variegata* male and female flowers at different developmental periods.

Conclusion

In this study, we used the male and female flowers of *S. variegata* at three developmental stages as materials and combined the transcriptome and metabolites to focus on the regulation of key metabolites that may be involved in the DEGs during the development of the flowers of this species. The study of the molecular mechanisms underlying the development of the flowers of *S. variegata*, which is a typical dioecious plant with important ecological restoration and levee-control plant, will enable us to better understand the adaptive evolution of its adaptive evolution of the breeding system. The results of these studies can also provide candidate genes and the theoretical basis of metabolism for the further utilization of molecular biology to regulate the accumulation of secondary metabolites in male and female flowers of *S. variegata*. Our results will contribute to understanding of the molecular and genetic mechanisms of male and female flower development in typical dioecious plants.

Materials and methods

Materials and pre-treatment

The samples for this study were collected from the riverside of Jingangbei, Beibei District, Chongqing, China (106.42092155°E, 29.84939019°N). The plant species was identified by Professor Hongping Deng. Its voucher specimen was deposited in the botanical herbarium of Southwest University (Holotype: SWCTU!) under voucher number Sva2023081901. Based on the bloom stage of *S. variegata* male and female flowers, samples of flower buds (male and female flowers were wrapped in the bud, F1/M1), full bloom stage (the stigmas / filaments were fully unfolded, F2/M2), final bloom stage (stigma pollination was completed / anther powder finished) were collected in July 2023 (Supplementary Fig. S5). At each developmental stage of the investigated female and male flowers, three replicates each were taken immediately frozen in liquid nitrogen and stored at -80 °C for transcriptome analysis by RNA-seq and six replicates were stored at -80 °C for metabolite identification (Supplementary Table S5-S6). The plants collected in this study and the subsequent experiments performed were in line with the IUCN Policy Statement on Research Involving Species at Risk of Extinction and the Convention on the Study Trade in Endangered Species of Wild Fauna and Flora. The plants were collected strictly following the provisions of the Regulations of the People's Republic of China on the Protection of Wild Plants, and a collection permit was obtained.

Transcriptomic analysis

A cDNA library from three developmental stages of male and female flowers of *S. variegata* was constructed for RNA-seq. The DNBSEQ-T24 sequencing platform was utilized for sequencing. The *S. variegata* genome was selected as a reference (Genome data are available in the National Genomics Data Center with the project number PRJCA026796). Gene expression levels were quantified in terms of exon model per kilobase per million mapped fragments (FPKM) values. DEGs were screened using DESeq2 and adjusted p-value and fold change. DEG enrichment was assessed based on comparisons with Gene Ontology (GO) and KEGG data⁶⁹. TFs were annotated using iTAK software and all TFs were obtained by BLAST search using Plant TFDB.

Metabolomics analysis

Untargeted metabolites were determined in male and female flowers of *S. variegata* using liquid chromatography-tandem mass spectrometry (LC-MS/MS) platform (Biomarker.

Technologies Co., Ltd.). The powder flower samples were weighed into 50 mg, and 1000 µL of the extraction liquid (methanol: acetonitrile: water v/v/v = 2:2:1) containing 20 mg/L internal standard (2-Chloro-L-phenylalanine) was added, vortexed, and mixed for 30 s. The samples were ground and sonicated in an ice-water bath for 10 min and then allowed to stand at -20 °C for 1 h. The results were summarized as follows: (a) The extract was analyzed by LC-MS/MS. After multiple centrifugations, the supernatant was taken to mix the QC samples in preparation for online testing. LC-MS on a Waters UPLC Acquity I-Class PLUS (Waters Corporation, Milford, CT, USA) and a Waters UPLC Xevo G2-XS QTOF (Waters Corporation, Milford, CT, USA) were used to analyze the sample extracts. The detected peak area information was normalized for subsequent analysis. The reproducibility of within-group and quantitative control samples was examined using principal component analysis. The identified compounds were categorized and pathway information was retrieved in databases such as KEGG, HMDB, and lipidmaps, the multiplicity of differences was calculated and compared based on the grouping information, and the t-test was utilized to calculate the significance of the difference p-value for each compound. The OPLS-DA modeling was performed using the R language package *ropes*, and the reliability of the model was verified by 200 substitution tests. DEMs were screened by combining the multiplicity of differences, p-value, and VIP value of the OPLS-DA model. The screening criteria were $FC \geq 1$, $P\text{-value} \leq 0.01$, and $VIP \geq 1$. A hypergeometric distribution test was utilized to calculate the differential metabolites with KEGG pathway enrichment significance.

Integrated transcriptome and metabolome analysis

Transcriptome and metabolome integrated correlation analysis was performed using using MetaboAnalyst 5.0⁷⁰. WGCNA analysis of genes associated with important DEMs was performed using the WGCNA package in R software⁷¹. A weighted neighborhood connectivity matrix between different genes was constructed using power functions, and similar modules in the hierarchical tree were filtered using a dynamic tree-cutting procedure. Pearson correlation analysis of DEGs and DEMs was performed based on the R package. Gene and metabolite relationship networks were visualized by Cytoscape_v3.9.1.

Validation of transcriptomic data

To examine the validity of the transcriptome data, 18 DEGs were randomly selected for quantification at three flowering stages in both male and female flowers of *S. variegata*. Total RNA was extracted using the TRIzol kit (Invitrogen, CA, USA) and cDNA was synthesized using Goldenstar RT6 cDNA Synthesis Mix (TSK314S) according to the maker's instructions. The *type 2 A phosphatase activator TIP41* (*TIP41*: Sva09G007630) gene was used as an internal control. All experiments were repeated at least 3 times.

Data availability

Transcriptome data were uploaded to GenBank under BioProject PRJNA1119374 (BioSample accessions SRR29274790 - SRR29274807). Metabolome data are available in Metabolome data are available in MetaboLights (www.ebi.ac.uk/metabolights), MTBLS10369. And other data is provided within the manuscript or supplementary information files.

Received: 13 November 2024; Accepted: 19 February 2025

Published online: 07 March 2025

References

- Vita, F. et al. Tuberomics: a molecular profiling for the adaption of edible fungi (*Tuber magnatum Pico*) to different natural environments. *BMC Genom.* **21** (1), 90 (2020).
- Jeyasri, R. et al. An overview of abiotic stress in cereal crops: negative impacts, regulation, biotechnology and integrated omics. *Plants* **10** (7), 1472 (2021).
- Wang, S. et al. Multi-omics analysis to visualize the dynamic roles of defense genes in the response of tea plants to Gray blight. *Plant. J.* **106** (3), 862–875 (2021).
- Feng, G. Y. Genome assembly and elaboration on the flowering regulation in orchardgrass. Dissertation (Sichuan Agriculture University, 2019).
- Wu, Y. Floral bud transcriptome analysis and research on floral development regulation mechanism of *Sapium sebiferum*. Dissertation (University of Science and Technology of China, 2015).
- Riechmann, J. L. & Ratcliffe, O. J. A genomic perspective on plant transcription factors. *Curr. Opin. Plant. Biol.* **3** (5), 423–434 (2000).
- Liu, Y. W., Li, X., Li, K. & Liu, H. T. Multiple bHLH proteins form heterodimers to mediate CRY2-dependent regulation of flowering-time in Arabidopsis. *Plos Genet.* **9** (10), e1003861 (2013).
- Ó'Maoláidigh, D. S., Graciet, E. & Wellmer, F. Gene networks controlling *Arabidopsis thaliana* flower development. *New. Phytol.* **201** (1), 16–30 (2014).
- Abe, M. et al. FE, a phloem-specific Myb-related protein, promotes flowering through transcriptional activation of FLOWERING LOCUS T and FLOWERING LOCUS T INTERACTING PROTEIN 1. *Plant. J.* **83** (6), 1059–1068 (2015).
- Xie, Y. et al. FHY3 and FAR1 integrate light signals with the miR156-SPL module-mediated aging pathway to regulate Arabidopsis flowering. *Mol. Plant.* **13** (3), 483–498 (2020).
- Saidi, A. & Hajibarat, Z. Computational study of environmental stress-related transcription factor binding sites in the promoter regions of maize auxin response factor (ARF) gene family. *Not Sci. Biol.* **12**, 646–657 (2020).
- Guan, Y. et al. Over expression of the CmJAZ1-like gene delays flowering in *Chrysanthemum morifolium*. *Hortic. Res.* **8** (1), 87 (2021).
- Luo, F. L., Zeng, B., Chen, T., Ye, X. Q. & Liu, D. Response to simulated flooding of photosynthesis and growth of riparian plant *Salix variegata* in the three Gorges reservoir region of China. *J. Plant. Ecol.* **31** (5), 910–918 (2007).
- Wobbe, L. The molecular function of plant mTERFs as key regulators of organellar gene expression. *Plant. Cell. Physiol.* **61** (12), 2004–2017 (2021).
- Chen, H. C. et al. Effects of exogenous organic acids on the characteristics of Cd accumulation of *Salix variegata* under Cd stress. *J. Plant. Ecol.* **32** (12), 4510–4518 (2019).
- Wang, Y., Wu, J. Q., Huang, H. W. & Liu, S. B. Quantitative analysis of plant communities in water level-fluctuation zone within three Gorges reservoir area of Changjiang river. *J. Wuhan Bot. Res.* **22** (4), 307–314 (2004).
- Bailey-Serres, J. & Voesenek, L. A. Flooding stress: Acclimations and genetic diversity. *Annu. Rev. Plant. Biol.* **59**, 313–339 (2008).
- Raulings, E., Morris, K., Roache, M. & Boon, P. I. The importance of water regimes operating at small spatial scales for the diversity and structure of wetland vegetation. *Freshw. Biol.* **55**, 701–715 (2010).
- Mcgowan, S. et al. Interdecadal declines in flood frequency increase primary production in lakes of a Northern river delta. *Global Change Biol.* **17** (2), 1212–1224 (2011).
- Chen, T., Zeng, B., Ye, X. Q., Luo, F. L. & Liu, D. Effect of flooding on adventitious root formation of *Arundinella anomala* Steud. And *Salix variegata* Franch. *J. Anhui Agric. Sci.* **35** (19), 5703–5704 (2007).
- Su, X. L., Zeng, B., Qiao, P., Qyi, Q. L. & Huang, W. J. The effects of winter water submergence on flowering phenology and reproductive allocation of *Salix variegata* Franch. In the Gorges reservoir region. *Sheng Tai Xue Bao.* **30** (10), 2585–25932 (2010).
- Zeng, C. C. et al. Effects of *Salix variegata* on soil microorganisms and enzymatic activity in contaminated soils under flooding conditions. *Sheng Tai Xue Bao.* **37** (13), 4327–4334 (2017).
- Li, R., Chen, J. P., Chen, H. C. & Ma, W. C. Cadmium distribution in the subcellular fractions of *Salix variegata* under flooding conditions. *Sheng Tai Xue Bao.* **38** (1), 186–194 (2018).
- Liu, Y., Wei, H., Ma, W. C. & Zhang, W. Accumulation and subcellular distribution of cadmium in *Salix variegata*. *Linye Kexue.* **54** (08), 48–55 (2018).
- Zhang, Q. et al. Integrative transcriptomic and metabolomic analyses provide insight into the long-term submergence response mechanisms of young *Salix variegata* stems. *Planta* **253** (5), 88 (2021).
- Shi, Y. Study on spatial distribution and regeneration capacity of woody plants in riparian zone of Central Districts of Chongqing. Dissertation (Southwest University, 2020).
- Qi, Y. C., Zhou, C., He, X. R., Wang, P. & Wei, H. Effects of exogenous organic acids on Cd forms in soil and Cd accumulation in *Salix variegata* Franch. *Res. Env. Sci.* **34** (9), 2220–2227 (2021).
- Ayi, Q. et al. Seed sojourn and fast viability loss constrain seedling production of a prominent riparian protection plant *Salix variegata* Franch. *Sci. Rep.* **6**, 37312 (2016).
- Wellmer, F. et al. Flower development: open questions and future directions. *Methods Mol. Biol.* **1110**, 103–124 (2014).
- Ding, Y., Shi, Y. & Yang, S. Molecular regulation of plant responses to environmental temperatures. *Mol. Plant.* **13** (4), 544–564 (2020).
- Namdar, D. et al. LED lighting affects the composition and biological activity of *Cannabis sativa* secondary metabolites. *Ind. Crop Prod.* **132**, 177–185 (2019).

32. Yang, B. et al. Integrative omics of *Lonicera japonica* thunb. Flower development unravels molecular changes regulating secondary metabolites. *J. Proteom.* **208**, 103470 (2019).
33. Meng, L. Functional characterization of Tg WRKY75 and Tg NAC29 during petal senescence in *Tulipa gesneriana*. Dissertation (Huazhong Agricultural University, 2022).
34. Theißen, G., Melzer, R. & Rümpler, F. MADS-domain transcription factors and the floral quartet model of flower development: linking plant development and evolution. *Development* **143** (18), 3259–3271 (2016).
35. Yao, J. L., Kang, C., Gu, C. & Gleave, A. P. The roles of floral organ genes in regulating Rosaceae fruit development. *Front. Plant. Sci.* **12**, 644424 (2022).
36. Fatima, M., Ma, X., Zhang, J. & Ming, R. Genome-wide analysis of MADS-box genes and their expression patterns in unisexual flower development in dioecious spinach. *Sci. Rep.* **14** (1), 18635 (2024).
37. Grimplet, J., Martinez-Zapater, J. M. & Carmona, M. J. Structural and functional annotation of the MADS-box transcription factor family in grapevine. *BMC Genom.* **17** (1), 80 (2016).
38. Cucinotta, M., Cavalleri, A., Chandler, J. W. & Colombo, L. Auxin and flower development: A blossoming field. *CSH Perspect. Bio.* **13** (2), a039974 (2021).
39. Pimenta Lange, M. J. & Lange, T. Ovary-derived precursor Gibberellin A9 is essential for female flower development in cucumber. *Development* **143** (23), 4425–4429 (2016).
40. Colquhoun, T. A. et al. G. EOBII controls flower opening by functioning as a general transcriptomic switch. *Plant. Physiol.* **156** (2), 974–984 (2011).
41. Schubert, R. et al. Tomato MYB21 acts in ovules to mediate Jasmonate-Regulated fertility. *Plant. Cell.* **31** (5), 1043–1062 (2019).
42. Yarahmadov, T., Robinson, S., Hanemian, M., Pulver, V. & Kuhlmeier, C. Identification of transcription factors controlling floral morphology in wild Petunia species with contrasting pollination syndromes. *Plant. J.* **104** (2), 289–301 (2020).
43. Zhang, X., He, Y., Li, L., Liu, H. & Hong, G. Involvement of the R2R3-MYB transcription factor MYB21 and its homologs in regulating flavonol accumulation in Arabidopsis stamen. *J. Exp. Bot.* **72** (12), 4319–4332 (2021).
44. Chen, W. H., Li, P. F., Chen, M. K., Lee, Y. I. & Yang, C. H. FOREVER YOUNG FLOWER negatively regulates ethylene response DNA-Binding factors by activating an ethylene-Responsive factor to control Arabidopsis floral organ senescence and abscission. *Plant. Physiol.* **168** (4), 1666–1683 (2015).
45. Yuan, Y. et al. Genetic variation and metabolic pathway intricacy govern the active compound content and quality of the Chinese medicinal plant *Lonicera japonica* thunb. *BMC Genom.* **13**, 195 (2012).
46. Olsen, A. N., Ernst, H. A., Leggio, L. L. & Skriver, K. NAC transcription factors: structurally distinct, functionally diverse. *Trends Plant. Sci.* **10** (2), 79–87 (2005).
47. Goeckeritz, C. & Hollender, C. A. There is more to flowering than those DAM genes: the biology behind bloom in rosaceous fruit trees. *Curr. Opin. Plant. Biol.* **59**, 101995 (2021).
48. Quiroz, S. et al. Beyond the genetic pathways, flowering regulation complexity in *Arabidopsis thaliana*. *Int. J. Mol. Sci.* **22** (11), 5716 (2021).
49. Li, P. et al. Integration of genome and transcriptome reveal molecular regulation mechanism of early flowering trait in *Prunus* genus (*Prunus Mume* and *Prunus persica*). *Front. Plant. Sci.* **13**, 1036221 (2022).
50. Salem, T. et al. Mutations in two putative phosphorylation motifs in the tomato pollen receptor kinase LePRK2 show antagonistic effects on pollen tube length. *J. Biol. Chem.* **286** (6), 4882–4891 (2011).
51. Boisson-Dernier, A. et al. Disruption of the pollen-expressed FERONIA homologs ANXUR1 and ANXUR2 triggers pollen tube discharge. *Development* **136** (19), 3279–3288 (2009).
52. Sun, L. et al. ZmHSP16.9, a cytosolic class I small heat shock protein in maize (*Zea mays*), confers heat tolerance in transgenic tobacco. *Plant. Cell. Rep.* **31** (8), 1473–1484 (2012).
53. Fan, M. et al. ZmSTK1 and ZmSTK2, encoding receptor-like cytoplasmic kinase, are involved in maize pollen development with additive effect. *Plant. Biotechnol. J.* **16** (8), 1402–1414 (2018).
54. Muhlemann, J. K. et al. Developmental changes in the metabolic network of snapdragon flowers. *PLoS One.* **7** (7), e40381 (2012).
55. Borghi, M. & Fernie, A. R. Floral metabolism of sugars and amino acids: implications for pollinators' preferences and seed and fruit set. *Plant. Physiol.* **175** (4), 1510–1524 (2017).
56. Vogt, T. Phenylpropanoid biosynthesis. *Mol. Plant.* **3** (1), 2–20 (2010).
57. Klisurova, D. et al. Co-Pigmentation of black chokeberry (*Aronia melanocarpa*) anthocyanins with phenolic co-pigments and herbal extracts. *Food Chem.* **279**, 162–170 (2019).
58. Zhang, C. et al. An integrated transcriptome and metabolome analysis reveals the gene network regulating flower development in *Pogostemon cablin*. *Front. Plant. Sci.* **14**, 1201486 (2023).
59. del Baño, M. J. et al. Phenolic diterpenes, flavones, and Rosmarinic acid distribution during the development of leaves, flowers, stems, and roots of *Rosmarinus officinalis*. Antioxidant activity. *J. Agric. Food Chem.* **51** (15), 4247–4253 (2003).
60. Li, M. et al. Molecular and biochemical characterization of two 4-coumarate: coa ligase genes in tea plant (*Camellia sinensis*). *Plant. Mol. Biol.* **109**, 579–593 (2022).
61. Ahmad, N. et al. Molecular and biochemical rhythms in dihydroflavonol 4-reductase-mediated regulation of Leucoanthocyanidin biosynthesis in *Carthamus tinctorius* L. *Ind. Crops Prod.* **156**, 112838 (2020).
62. Davière, J. M. & Achard, P. A pivotal role of DELL as in regulating multiple hormone signals. *Mol. Plant.* **9** (1), 10–20 (2016).
63. Hu, J. et al. Potential sites of bioactive Gibberellin production during reproductive growth in Arabidopsis. *Plant. Cell.* **20** (2), 320–336 (2008).
64. Bush, S. M. & Krysan, P. J. Mutational evidence that the Arabidopsis MAP kinase MPK6 is involved in anther, inflorescence, and embryo development. *J. Exp. Bot.* **58**, 2181–2191 (2007).
65. Vieira Dos Santos, C., Cuiné, S., Rouhier, N. & Rey, P. The Arabidopsis plastidic methionine sulfoxide reductase B proteins. Sequence and activity characteristics, comparison of the expression with plastidic methionine sulfoxide reductase A, and induction by photooxidative stress. *Plant. Physiol.* **138** (2), 909–922 (2005).
66. Sheren, J. E. & Kassenbrock, C. K. RNF38 encodes a nuclear ubiquitin protein ligase that modifies p53. *Biochem. Biophys. Res. Commun.* **440** (4), 473–478 (2013).
67. Nomura, T., Ogita, S. & Kato, Y. A novel lactone-forming carboxylesterase: molecular identification of a Tuliposide A-converting enzyme in tulip. *Plant. Physiol.* **159** (2), 565–578 (2012).
68. Ramakrishnan, M. et al. Selenium: a potent regulator of ferroptosis and biomass production. *Chemosphere* **306**, 135531 (2022).
69. Love, M. I., Huber, W. & Anders, S. Moderated Estimation of fold change and dispersion for RNA-seq data with DESeq2. *Genome Biol.* **15** (12), 550 (2014).
70. Pang, Z. et al. MetaboAnalyst 5.0: narrowing the gap between Raw spectra and functional insights. *Nucleic Acids Res.* **49** (W1), W388–W396 (2021).
71. Khan, I. A. et al. Identification of key gene networks controlling anthocyanin biosynthesis in Peach flower. *Plant. Sci.* **316**, 111151 (2022).

Acknowledgements

This work was supported by the Central Forestry Reform and Development Fund-National Key Protected Wild-life Protection Project (zlg2021-cq20211210) and (zlg2022-cq20220907). We would like to thank the editor and

reviewers for their helpful comments and suggestions on the manuscript. We would like to thank Biomarker Technologies CO., LTD (Beijing, China) and UW Genetics (Wuhan, China) for their help with data processing, respectively.

Author contributions

H.P. D. conceived, designed, and supervised the research project. H. Z., X. Z., R. P., M.W. T., Y. P., and Y.Y. W. performed the experiments. H. Z., W.Q. L., and X. Z. analyzed the data. H. Z. wrote the manuscript. W.Q. L. and X. Z. provided input on the data presentation. Y.W. Z. revised the manuscript. All authors contributed to the article and approved the submitted version.

Declarations

Competing interests

The authors declare no competing interests.

Additional information

Supplementary Information The online version contains supplementary material available at <https://doi.org/10.1038/s41598-025-91317-0>.

Correspondence and requests for materials should be addressed to H.D.

Reprints and permissions information is available at www.nature.com/reprints.

Publisher's note Springer Nature remains neutral with regard to jurisdictional claims in published maps and institutional affiliations.

Open Access This article is licensed under a Creative Commons Attribution-NonCommercial-NoDerivatives 4.0 International License, which permits any non-commercial use, sharing, distribution and reproduction in any medium or format, as long as you give appropriate credit to the original author(s) and the source, provide a link to the Creative Commons licence, and indicate if you modified the licensed material. You do not have permission under this licence to share adapted material derived from this article or parts of it. The images or other third party material in this article are included in the article's Creative Commons licence, unless indicated otherwise in a credit line to the material. If material is not included in the article's Creative Commons licence and your intended use is not permitted by statutory regulation or exceeds the permitted use, you will need to obtain permission directly from the copyright holder. To view a copy of this licence, visit <http://creativecommons.org/licenses/by-nc-nd/4.0/>.

© The Author(s) 2025